Exploration of the Mechanism of the Hydrolysis of Chlorine Nitrate in Small Water Clusters Using Electronic Structure Methods

Jonathan P. McNamara and Ian H. Hillier*

Department of Chemistry, University of Manchester, Manchester, M13 9PL, U.K.

Received: April 2, 1999; In Final Form: July 1, 1999

High-level electronic structure calculations have been used to study the mechanism of hydrolysis of chlorine nitrate in neutral water clusters containing three to eight solvating water molecules. The calculations clarify some of the current uncertainties in the hydrolysis mechanism. As the size of the water cluster is increased, $ClONO_2$ shows increasing ionization along the O_2NO-Cl bond consistent with the proposed *predissociation* in which the electrophilicity of the chlorine atom is enhanced, thus making it more susceptible to nucleophilic attack from a surface water molecule. A species akin to the experimentally observed intermediate, H_2OCl^+ is found to be stable in a cluster containing eight water molecules. The hydrolysis products, ionized nitric (H_3O^+/NO_3^-) and molecular hypochlorous (HOCl) acids, are found to be stable in two different types of structures, containing six and eight water molecules. For the water cluster containing six water molecules, which has a structure related to ordinary hexagonal ice, $ClONO_2$ is hydrolyzed to yield H_3O^+/NO_3^-/HOCl, with essentially no barrier. The calculations thus predict that hydrolysis of $ClONO_2$ on PSC ice aerosols can proceed spontaneously in small neutral water clusters.

1. Introduction

The heterogeneous chemistry of $ClONO_2$ on polar stratospheric cloud particles (PSC's) has been isolated as a major contributor to stratospheric ozone depletion over Antarctica.[1−12] During the Antarctic winter, surface-catalyzed reactions convert reservoir species $ClONO_2$ and HCl to Cl_2 and HOCl. These species are then photolyzed in the spring to produce Cl radicals involved in the catalytic depletion of ozone. PSC ice aerosols, the sites for the transformation of reservoir species, generally consist of two types, type I, nitric acid trihydrates (NAT), or type II, water ice.

The activation of $ClONO_2$ can occur via a two-step mechanism (eqs 1a and 1b) producing hypochlorous and nitric acids, or by a direct mechanism (eq 2).

$$ClONO_2 + H_2O \rightarrow HOCl + HONO_2 \quad (1a)$$

$$HOCl + HCl \rightarrow Cl_2 + H_2O \quad (1b)$$

$$ClONO_2 + HCl \rightarrow Cl_2 + HONO_2 \quad (2)$$

The hydrolysis reaction has been extensively studied experimentally using the complementary techniques of Fourier transform (FTIR) or reflection−absorption (RAIR) infrared spectroscopy and mass spectrometric (MS) methods.[13−17] FTIR and RAIR spectroscopy allow for some direct observation and discrimination of different surface adsorbed species, reactants or products, while MS methods allow the determination of products evolved from surfaces.[13−17] Modern laboratory apparatus also allows the control of other experimental parameters such as reactant partial pressure and substrate temperature so that conditions close to stratospheric ones can be simulated. Measurements of reaction probabilities or *sticking coefficients*, γ, using flow tubes have been developed by Hanson,[18−21] Zhang,[22,23] and other workers.[24−29] Methods to study the interaction of $ClONO_2$ with ion-containing water clusters[30−32] and kinetic studies[33] are also well documented.

Hanson[34] studied the reactive uptake of $ClONO_2$ on ^{18}O-labeled ice. He found that the hypochlorous acid (eq 1a) contained ^{18}O, indicating that the $Cl-ONO_2$ bond was broken during hydrolysis. This finding thus suggests an alternative mechanism to the acid catalysis proposed by Wofsy et al.[35] and Nelson and Okumura.[30] On the basis of Hanson's findings and previous theoretical work[36,37] (see later), it is widely accepted that the strongest interaction of $ClONO_2$ with water occurs at the chlorine atom. Calculations indicating the polarized nature of the chlorine nitrate molecule,[36] suggest that chlorine is the most accessible electrophilic site and is thus susceptible to nucleophilic attack[36] by surface adsorbed species[13−17] in this way. Thus, the reactivity of $ClONO_2$ is controlled by the relative nucleophilic/electrophilic strengths of the species involved.

However, there are still three mechanistic issues that have yet to be completely clarified by experiment or theoretical methods,[38] which we address in this work.

(i) The *predissociation* or *ionization* of chlorine nitrate along the O_2NO-Cl bond serving to increase the electrophilicity of the Cl atom, particularly the role of water in enhancing this effect.[16,17]

(ii) The existence, or otherwise, of the ion H_2OCl^+.[13−15]

(iii) Whether the product nitric acid is in its *ionic* or *molecular* form.[13−17]

Although there have been many experimental studies[13−35] of the atmospheric chemistry of chlorine nitrate, in particular the hydrolysis reaction, there have been only a limited number of theoretical studies,[36−43] and current uncertainties in the mechanism of hydrolysis remain. Lee determined geometries and harmonic frequencies of free $ClONO_2$[41] and studied the protonation reaction of $ClONO_2$[42] (proposed by Wofsy et al.[35]) at the CCSD(T) level. Ying and Zhao[37] also calculated geometries and harmonic frequencies using density functional theory, in agreement with Lee and La Manna's[36] results. Early ab initio investigations of the hydrolysis of chlorine nitrate focused on its interaction with single water molecules. La Manna studied

10.1021/jp991137i CCC: $18.00
Published on Web 08/20/1999

six isomers of $ClNO_3$ at the Hartree−Fock and MP2 levels and proposed that the likely coordinate for hydrolysis was the Cl···O intermolecular axis. On the mechanistic side, Bianco and Hynes[38] have studied the hydrolysis reaction using a $(H_2O)_3$ cluster and Hartree−Fock theory. The reaction products were the molecular acids, HOCl and $HONO_2$. The activation barrier was calculated to be ca. 25 kcal mol^{-1}, which is clearly too high to account for the ready reaction on ice. On the basis of experimental evidence, such a mechanism is suggested to be applicable to temperatures lower than those of the stratosphere, under a reduced water regime.[16] Akhmatskaya et al.[39] have calculated a barrier of 44.7 kcal mol^{-1} for the hydrolysis reaction via Hanson's proposed transition state,[34] involving a single water molecule. Other important atmospheric reactions have also been studied using ab initio methods.[44−51]

In this paper, we present the results of density functional calculations in order to understand the reactivity of chlorine nitrate on PSC ice aerosols. The current uncertainties in the hydrolysis mechanism are addressed by cluster models, in which we investigate the importance and extent to which predissociation occurs in hydrolysis.[16,17] We also study the possibility of the existence of the experimentally proposed H_2OCl^+ intermediate.[13−15] In any study, it is important to provide a link between theoretical results and experiment. For this reason, we have chosen to calculate vibrational frequencies for all our structures in order to draw comparisons with the available experimental IR data.[13−17] A model reaction system is also presented in which the structural arrangement of the water molecules is strongly related to that of a hexagonal ice crystal. In our mechanistic study, we confirm the experimental observations that at stratospherically relevant temperatures the final reaction products contain the ionized form of nitric acid, $H_3O^+NO_3^-$.[13−17] The activation barrier of the hydrolysis reaction is found to be very small, in line with physical−chemical models[52] and is consistent with the expected fast reaction on ice. Finally, in light of our calculations, the implications for stratospheric chemistry are discussed.

2. Modeling the Ice Surface

The surface structure of ordinary hexagonal ice is generally unknown. Hexagonal ice is formed when liquid water freezes at atmospheric pressure, where the oxygen atoms comprise a wurzite lattice.[53] The hydrogen atoms are distributed throughout the lattice along the O−O bonds according to the Bernal and Fowler ice rules.[54] The disorder in the proton positions exists down to 0 K and is responsible for the residual entropy at this temperature.[55] Another form, cubic ice, also exists and is formed by condensation of water vapor below −80 °C.[53] Cubic ice has a similar structure to hexagonal ice, except the oxygen positions occupy a diamond lattice. The hydrogen positions are also disordered within the Bernal and Fowler ice rules.[54]

Experimentally the ice surface has been probed using a variety of techniques. Materer et al.[56] crystallized an ice film on a Pt(111) surface at 90 K. The structure of the external surface was investigated using LEED, molecular dynamics, and ab initio calculations. They found that the ice surface had full bilayer termination (refer to Figure 1). Devlin and Buch have used FTIR spectroscopy and molecular dynamics/Monte Carlo simulations to investigate the ice surface.[57−62] They have used a novel technique which uses small adsorbate molecules such as CF_4 to probe the surface structure by observing shifts in surface localized vibrational modes, due to the presence of the adsorbate. By comparison with simulation, they assign surface molecules to one of three categories: three-coordinated molecules with either dangling hydrogen or dangling oxygen coordination and four-coordinated molecules with distorted tetrahedral geometry. Buch et al.[62] also note that both simulation and experiment indicate that the surface of ice contains rings of water molecules large enough to accommodate several adsorbate species.

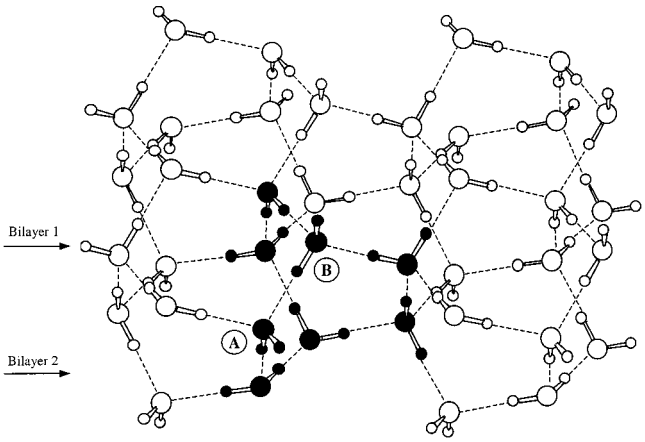

Figure 1. Fragment of proton ordered hexagonal ice, showing water molecules (A, B) removed to accommodate chlorine nitrate.

Theoretical studies have tended to concentrate on the bulk properties of crystals rather than the surface.[53,55,63−66] The interaction of small atmospherically relevant species such as HOCl and HCl with ice surfaces has been studied using high-level electronic structure methods.[44,45,48] Geiger et al.[44] have used a four-water cluster excised from the ideal surface of hexagonal ice. Similarly, Brown and Doren[45] have applied density functional theory to study the interaction of HOCl with $(H_2O)_4$ and $(H_2O)_{26}$ cluster models excised from the (0001) surface of hexagonal ice. The latter models were constrained in order to retain the structural properties of the unrelaxed ice surface. Alternatively, atmospherically relevant reactions have been studied using small water clusters and ab initio methods. Vincent et al.[50] have explored the mechanism of oxidation of sulfur dioxide and bisulfite by hydrogen peroxide in water droplets. Smith et al.[51] have used density functional methods to elucidate the mechanism of acid dissociation in water clusters and the cooperative nature of the ionization process.

Experimental evidence[57−62] would seem to suggest that on the ice surface there are a number of different adsorption sites. The simulations of CF_4 adsorbate uptake and spectra on model icy surfaces by Buch et al.[62] have important implications for the chemistry of ice surfaces. Experimental comparisons suggest that the annealed (140 K) nanocrystal surface is *relatively smooth* but *laterally disordered*, while the surface of the unannealed nanocrystals is *disordered and rough*.[62] Within the locality of the adsorption site, it is likely that there will be other surface-adsorbed species, in particular H_2O. Models that represent the local adsorption site by fragments excised from an ideal ice lattice[44,45] may not account for the solvating effect of the ice surface beyond the adsorption site. As the foreign molecule approaches the ice surface, there is a high probability that it will be at least partially solvated either by surface-bound H_2O or within a ring of water molecules.

In view of Buch's findings,[62] we have chosen to model the locality of the adsorption site for $ClONO_2$ hydrolysis by cluster models, where $ClONO_2$ is partially solvated by additional surface-bound H_2O molecules. These cluster models will be disordered as with the unannealed nanocrystal surface.[62] We also investigate the hydrolysis of $ClONO_2$ within a cluster that is excised from an ideal proton-ordered lattice (Figure 1).[55,63] This particular adsorption site is created by the removal of two

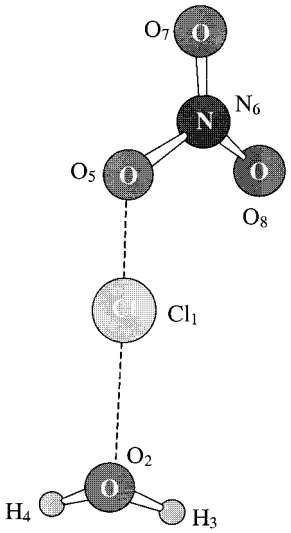

Figure 2. Core reaction system.

of the surface bilayer H_2O molecules, denoted A and B. The reactive site will have features characteristic of the proposed ring structures found on the annealed surface.

Finally, these models have been chosen based on experimental findings concerning the hydrolysis mechanism, where excess surface water promotes preionization and favors the formation of the solvated nitric acid.[13−17]

3. Computational Methods

All calculations reported have been carried out using the Gaussian 94[67] and Gaussian 98[68] suites of programs. Electron correlation has been included using density functional theory (B3LYP)[69−71] and Møller−Plesset perturbation theory (MP2).[72] The density functional method was chosen to minimize computational expense, MP2 optimizations being too time-consuming for systems having ca. 350 basis functions. We chose the flexible 6-311++G(d,p) basis set to obtain structures on the potential energy surface. Our choice of functional and basis set was guided by previous work. Ying and Zhao[37] found the B3LYP functional gave results of comparable quality to the CCSD/TZ2P method for isolated $ClONO_2$. Recent electronic structure calculations involving water clusters have shown that both polarization and diffuse functions are required to describe hydrogen-bonded systems.[50,51] Stationary structures were characterized as minima or transition structures on the potential energy surface by calculation of harmonic vibrational frequencies. Free energies were calculated within the perfect gas, rigid rotor, harmonic oscillator approximation at 180 K, a temperature appropriate to the experimental conditions.[13−17] These electronic structure calculations were particularly appropriate for the parallel version of Gaussian 94,[67] and a number of them were carried out on the CRAY T3E, of the CSAR Service at Manchester Computing.[73]

4. Computational Results

A. Stationary Structures. In discussing the various structures, we refer to the atomic numbering scheme of the core reaction system shown in Figure 2, which contains $ClONO_2$ and the attacking nucleophile, H_2O. The minimum energy structures of chlorine nitrate solvated by three, five, six, and eight water molecules are shown in Figures 3−9. All of the structures are denoted by the number of *complete* water molecules they contain *before* reaction. Individual structural parameters are at the B3LYP/6-311++G(d,p) level unless otherwise stated. Electronic and free energies of all structures are given in Table 1. When comparing the relative stabilities of our reactant and ion pair structures, we refer to the difference in free energy given in Table 1. The free energy of binding of $ClONO_2$ within our reactant structures is defined as the difference between the free energy of the optimized cluster containing $ClONO_2$ and the sum of the free energies for the isolated $ClONO_2$ and water cluster fragments. Finally, the gas-phase geometries of H_2O, HOCl, H_2OCl^+, H_3O^+, and NO_3^- are given in Table 2 for comparison.

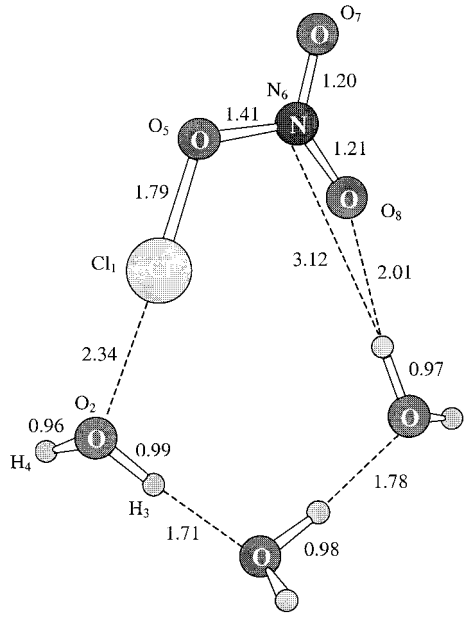

Figure 3. Reactant structure $ClONO_2 \cdot (H_2O)_3$ showing chlorine nitrate solvated by three water molecules. In this and subsequent figures, distances are in angstroms and correspond to the optimized B3LYP/6-311++G(d,p) geometries unless otherwise stated.

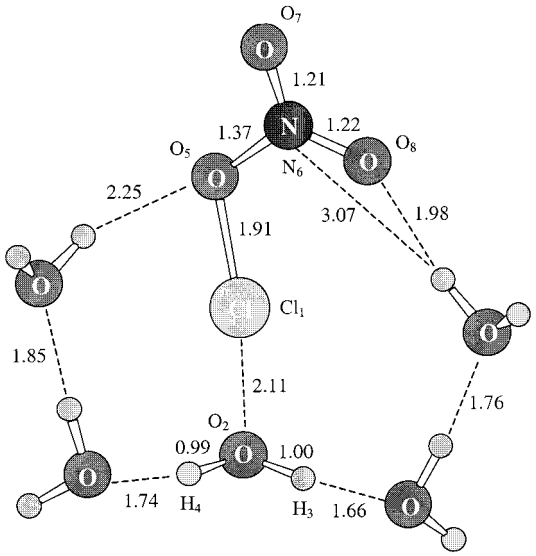

Figure 4. Reactant structure $ClONO_2 \cdot (H_2O)_5$ showing chlorine nitrate solvated by five water molecules.

Gas-Phase $ClONO_2$. First, we consider the gas-phase structure of chlorine nitrate. A theoretical study by La Manna[36] has shown $ClONO_2$ to be the lowest energy isomer of chlorine nitrate. Table 3 compares our calculated B3LYP/6-311++G(d,p) geometry with both a coupled cluster calculation and experiment.[41] The density functional theory (DFT) geometry is of comparable quality to the coupled cluster geometry and is in relatively good

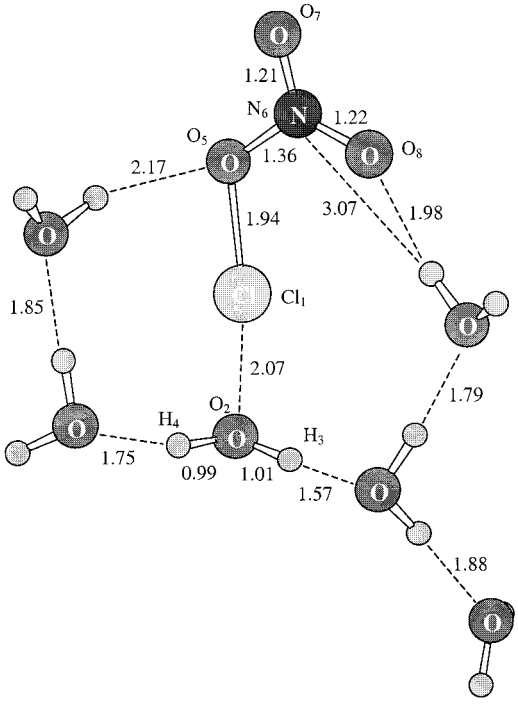

Figure 5. Reactant structure $ClONO_2 \cdot (H_2O)_6$ showing chlorine nitrate solvated by six water molecules (isomer 1).

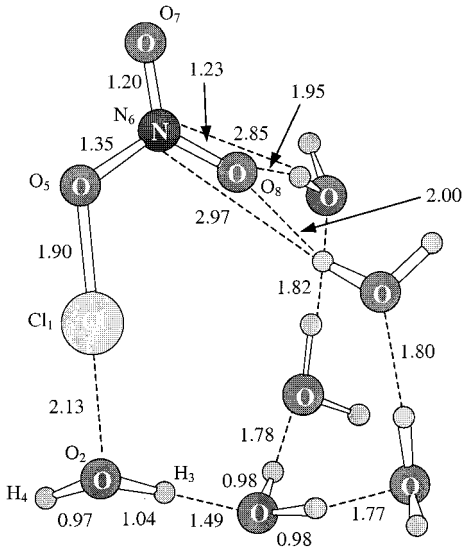

Figure 6. Reactant structure $ClONO_2 \cdot (H_2O)_6$ showing chlorine nitrate solvated by six water molecules (isomer 2).

agreement with experiment. The largest discrepancy occurs in the Cl_1-O_5 bond distance, the DFT geometry being in error by ca. 0.04 Å. Obermeyer[74] has studied the crystal structure of $ClONO_2$ at −166 °C. He interprets his results by considering $ClONO_2$ to consist of an NO_2 radical bonded to a ClO radical with a small negative charge on the NO_2 moiety. Experimentally,[41] the N_6-O_5 bond distance is found to be 1.499 Å, which is considerably longer than the other nitrate N−O bonds of length 1.196 Å and thus the structure differs from that of a regular *triangular* nitrate. The calculated Mulliken charges (Table 4) indicate that, in the isolated molecule, there is a polarization of charge, with a large negative charge of −0.26 on the nitrogen and a small positive charge on the chlorine of 0.08. Having briefly considered the gas-phase structure of chlorine nitrate, we can now consider the structural effects of solvating in three, five, six, and eight water molecules.

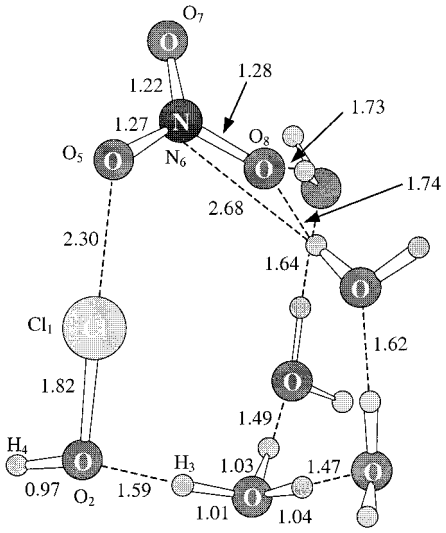

Figure 7. Ion pair structure $ClONO_2 \cdot (H_2O)_6$ showing solvated ionized nitric acid and molecular hypochlorous acid.

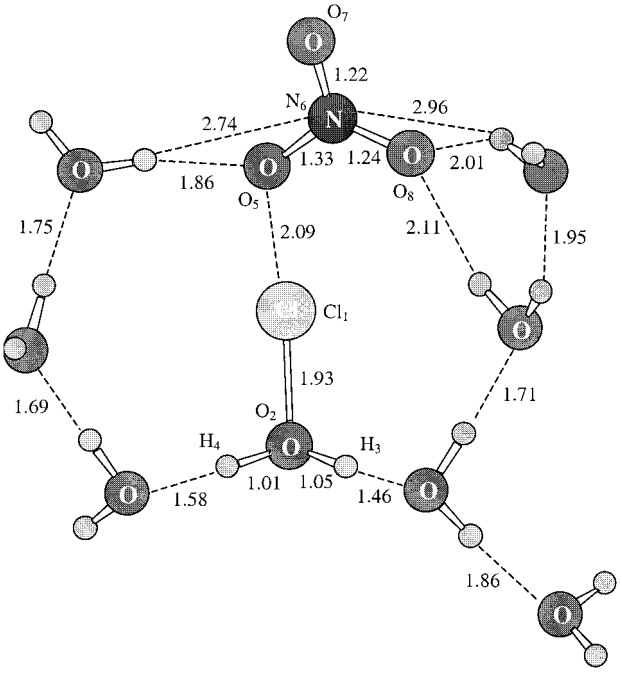

Figure 8. Ion pair structure $ClONO_2 \cdot (H_2O)_8$ showing solvated hypochlorous acidium and nitrate ions.

Reactant Structures. We have defined a *reactant structure* as a system in which the chlorine atom has *not* transferred to the attacking nucleophile, H_2O, such that the Cl_1-O_5 intramolecular distance is *less* than the Cl_1-O_2 intermolecular distance. Our reactant structures are shown in Figures 3−6 and illustrate four important trends. First, the addition of extra water molecules into the rings solvating chlorine nitrate causes a significant lengthening of the Cl_1-O_5 intramolecular distance and a shortening of the Cl_1-O_2 intermolecular distance, clearly showing the catalytic effect of the addition of water molecules. A shortening of the O_5-N_6 bond distance with the addition of water molecules is also noted. This observation is consistent with the chlorine nitrate ionizing towards $Cl^{\delta+}NO_3^{\delta-}$, during which the O_5-N_6 bond gains more *double bond character* as the nitrate anion is formed. The inclusion of extra solvating water molecules around $ClONO_2$ or the model cluster increases the binding energy of the adsorbate significantly (Table 1). Mulliken charges indicate significant charge transfer from

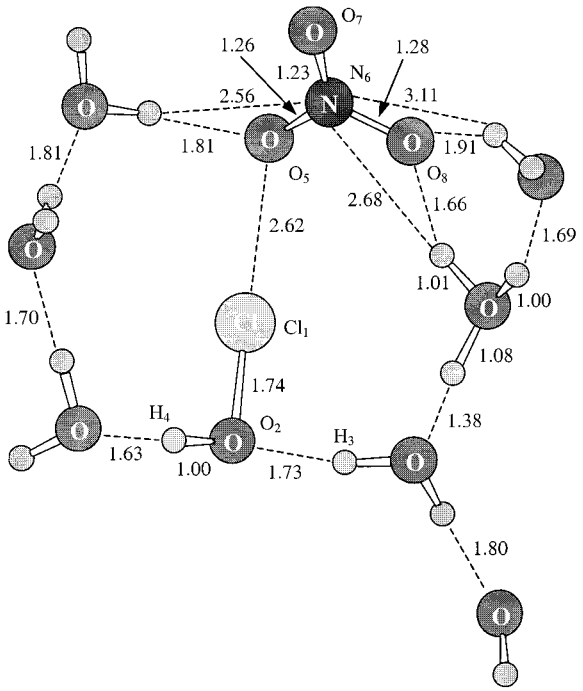

Figure 9. Ion pair structure $ClONO_2 \cdot (H_2O)_8$ showing solvated ionized nitric acid and molecular hypochlorous acid.

TABLE 1: Electronic and Free Energies (Hartrees) and Binding Free Energies of $ClONO_2$ (kcal mol^{-1}) of Reactant and Ion Pair Structures (at 180.0 K)

reactant structure	electronic energy	free energy	binding free energy of $ClONO_2$
$ClONO_2 \cdot (H_2O)_3$[a]	−969.943859	−969.874665	5.76
$ClONO_2 \cdot (H_2O)_5$[b]	−1122.888184	−1122.771762	22.10
$ClONO_2 \cdot (H_2O)_6$ (isomer 1)[c]	−1199.357185	−1199.219755	27.01
$ClONO_2 \cdot (H_2O)_6$ (isomer 2)[d]	−1199.360336	−1199.220408	23.12

ion pair structure	electronic energy	free energy
$ClONO_2 \cdot (H_2O)_6$ $(H_3O^+/NO_3^-/HOCl)$[e]	−1199.362400	−1199.220451
$ClONO_2 \cdot (H_2O)_8$ (H_2OCl^+/NO_3^-)[f]	−1352.307824	−1352.122628
$ClONO_2 \cdot (H_2O)_8$ $(H_3O^+/NO_3^-/HOCl)$[g]	−1352.310299	−1352.125048

[a] Figure 3. [b] Figure 4. [c] Figure 5. [d] Figure 6. [e] Figure 7. [f] Figure 8. [g] Figure 9.

TABLE 2: Calculated Bond Lengths (Å) and Angles (deg) of H_2O, HOCl, H_2OCl^+, H_3O^+, and NO_3^-

species	bond length	angle
H_2O	r(O−H) = 0.962	HOH = 105.1
HOCl	r(O−H) = 0.968	HOCl = 103.1
	r(O−Cl) = 1.731	
H_2OCl^+[a]	r(O−Cl) = 1.772	HOH = 123.9
	r(O−H) = 0.984	HOCl = 111.0
H_3O^+[a]	r(O−H) = 0.980	HOH = 113.5
NO_3^-[a]	r(O−N) = 1.260	ONO = 120.0

[a] For H_3O^+ and NO_3^-, internal O−H, O−N bonds and HOH, ONO angles are the same. Dihedrals omitted.

the attacking water to the $ClONO_2$ entity, increasing the ionic nature of the interaction as the number of waters in the solvating rings is increased (Table 4). Frontier molecular orbital theory has shown that there is efficient overlap between the HOMO of H_2O and the LUMO of $ClONO_2$, along the Cl_1-O_2 intermolecular axis, thus facilitating the charge transfer.[13]

TABLE 3: Geometric Parameters of $ClONO_2$

geom. parameters[a]	B3LYP/6-311++G(d,p)	CCSD(T)/TZ2P[b]	expt[c]
$r(Cl_1-O_5)$	1.711	1.707	1.673
$r(N_6-O_5)$	1.516	1.511	1.499
$r(N_6-O_7)$	1.189	1.197	1.196
$r(N_6-O_8)$	1.188	1.195	1.196
$\angle(Cl_1-O_5-N_6)$	113.9	111.9	113.0
$\angle(O_5-N_6-O_7)$	108.5	108.7	108.8
$\angle(O_5-N_6-O_8)$	117.6	117.8	118.6

[a] Bond lengths (Å), angles (deg), $ClONO_2$ is planar. Atomic numbering in Figure 2. [b] Lee.[41] [c] Vibrationally averaged gas-phase $ClONO_2$ structure.[41]

We believe these structures provide evidence for the proposed predissociation of chlorine nitrate, where ionization along the O_2NO-Cl bond serves to increase the electrophilicity of the chlorine atom, which is thus prone to nucleophilic attack from H_2O.[13−17] The important structural parameters and charge distributions of the reactant structures are now discussed.

$ClONO_2 \cdot (H_2O)_3$. Our initial model system contains chlorine nitrate solvated by three water molecules (Figure 3). A recent theoretical study by Bianco and Hynes[38] has used a similar cluster to investigate the hydrolysis of chlorine nitrate, where the three water molecules are structurally related to a fragment excised from a hexagonal ice lattice.[38]

The binding energy of chlorine nitrate to this model adsorption site is calculated to be 5.8 kcal mol^{-1} (Table 1). The $Cl-O_5$ intramolecular distance is 1.79 Å, which is a little longer than that calculated for gas-phase chlorine nitrate, 1.71 Å (Table 3). The O_5-N_6 bond length has shortened from 1.52 Å in the gas phase to 1.41 Å. By comparison with the gas-phase geometry of chlorine nitrate (Table 3), solvation by three water molecules promotes partial ionization of $ClONO_2$. Analysis of the Mulliken charges (Table 4) calculated for $ClONO_2$ within the $(H_2O)_3$ cluster indicate that the charge distribution is perturbed only a little compared to the isolated molecule. The charge on N_6 has become more negative, −0.32 (−0.26 free $ClONO_2$), and that on O_8 has decreased from 0.08 to −0.03, probably due to hydrogen bonding. Overall, charge is transferred to the $ClONO_2$ fragment, which now has a total charge of −0.16 (Table 4).

$ClONO_2 \cdot (H_2O)_5$. An additional *two bridging* water molecules have been added to the $(H_2O)_3$ system to form a $(H_2O)_5$ cluster, where the $ClONO_2$ entity is solvated by two water rings (Figure 4). In this model, the solvating environment has features evident of the 140 K annealed ice surface studied by Buch et al.[62] Combined simulation and experimental investigations suggest that, within the annealed surface, there are rings of water molecules large enough to accommodate several adsorbate species. A disordered ice surface[62] would also present the incoming adsorbate with a wide range of solvating environments, some of which may be able to partially surround the chlorine nitrate molecule, as in the $(H_2O)_5$ cluster.

Importantly, the inclusion of two more solvating water molecules has increased the binding energy of $ClONO_2$ by 16.3 kcal mol^{-1} to 22.1 kcal mol^{-1} (Table 1). The Cl_1-O_5 intramolecular distance has further increased to 1.91 Å from 1.79 Å in the $(H_2O)_3$ system. The formation of the nitrate anion as $ClONO_2$ ionizes is evident by the shortening of the O_5-N_6 bond length to 1.37 Å from 1.52 Å in the isolated molecule. The Mulliken charges for this reactant system indicate increased charge transfer from the attacking water to the chlorine nitrate entity (Table 4). The total atomic charge on $ClONO_2$ is −0.36, compared to −0.16 for the $(H_2O)_3$ reactant system. In parallel with this, the positive charge on the attacking water has

TABLE 4: Mulliken Charges (*e*) of Core Reactant System (Figure 2) in Reactant Structures

	atomic charge				
atom	$ClONO_2$	$ClONO_2 \cdot (H_2O)_3$[a]	$ClONO_2 \cdot (H_2O)_5$[b]	$ClONO_2 \cdot (H_2O)_6$[c] (isomer 1)	$ClONO_2 \cdot (H_2O)_6$[d] (isomer 2)
Cl_1	0.08	0.09	0.00	−0.01	0.06
O_2		−0.51	−0.43	−0.42	−0.47
H_3		0.37	0.40	0.42	0.44
H_4		0.27	0.35	0.34	0.28
O_5	0.07	0.09	0.01	−0.01	0.08
N_6	−0.26	−0.32	−0.30	−0.30	−0.38
O_7	0.03	0.01	0.00	−0.02	0.03
O_8	0.08	−0.03	−0.07	−0.08	−0.12
	total fragment charge				
fragment	$ClONO_2$	$ClONO_2 \cdot (H_2O)_3$[a]	$ClONO_2 \cdot (H_2O)_5$[b]	$ClONO_2 \cdot (H_2O)_6$[c] (isomer 1)	$ClONO_2 \cdot (H_2O)_6$[d] (isomer 2)
NO_3	−0.07	−0.25	−0.36	−0.41	−0.39
H_2O		0.13	0.32	0.34	0.25
$ClONO_2$	0.00	−0.16	−0.36	−0.42	−0.33

[a] Figure 3. [b] Figure 4. [c] Figure 5. [d] Figure 6.

increased by 0.19, from 0.13 for the $(H_2O)_3$ reactant system to 0.32 (Table 4).

$ClONO_2 \cdot (H_2O)_6$. We have examined two possible structures in which $ClONO_2$ is solvated with six water molecules. The first is isomer 1 (Figure 5), in which our $ClONO_2 \cdot (H_2O)_5$ structure is further solvated with an additional, extra-ring water molecule. Isomer 2 involves six water molecules in a structure related to ice and is shown in Figure 6.

Isomer 1. To our $(H_2O)_5$ system we have added a further remote water molecule to study the effect on ionization of a second solvation shell (Figure 5). Significantly, the inclusion of the extra water has increased the binding energy of $ClONO_2$ by 4.9 kcal mol^{-1} to 27.0 kcal mol^{-1} (Table 1). Again, increasing the number of solvating water molecules causes a lengthening of the Cl_1-O_5 intramolecular distance, in this case to 1.94 Å, a value greater than that found for other structures discussed so far. During the process of ionization, the transfer of chlorine is coupled to a lengthening of the O−H bond of the attacking water. In this structure, this effect is now evident from the lengthening of the O_2-H_3 bond to 1.01 Å from the value of 0.99 Å found in the $(H_2O)_3$ reactant system. Associated with these structural changes there is increased charge transfer from the attacking water to the chlorine nitrate (Table 4). $ClONO_2$ now has a net charge of −0.42 where essentially all of this charge is associated with the NO_3 moiety. A substantial positive charge of 0.34 is also associated with the H_2O nucleophile. Within this structure, the transferring chlorine is effectively neutral. We can conclude that waters in the second solvation shell do have an appreciable effect on the ionization process. The net effect of a full second solvation shell may further increase the extent of ionization.

Isomer 2. The second isomer (Figure 6) contains six water molecules structurally related to ordinary hexagonal ice. In hexagonal ice, the oxygen positions are ordered but the hydrogens are distributed throughout the lattice, along the O−O bonds, according to the Bernal and Fowler ice rules.[54] Figure 1 depicts a proton-ordered phase of hexagonal ice, with the model cluster water positions shown. Two of the surface bilayer water molecules (A, B) have been removed to produce the adsorption site for $ClONO_2$. By consideration of the work of Buch et al.,[62] our model system could be present either as part of a ring structure on the annealed nanocrystal surface or as surface defects found on the disordered unannealed surface.

The free energy (Table 1) of isomer 2 is ca. 0.4 kcal mol^{-1} lower than that of isomer 1. This small difference is not unexpected, since both isomers contain the same number of hydrogen bonds and *dangling* nonbonded hydrogens. The binding energy of $ClONO_2$ within the isomer 2 reactant structure is 23.1 kcal $mol,^{-1}$ which is 3.9 kcal mol^{-1} *less* than in the isomer 1 reactant structure.

Structurally, the intramolecular Cl_1-O_5 distance in isomer 2, 1.90 Å, is shorter than that in isomer 1 by 0.04 Å, although the O_2-H_3 bond length is 1.04 Å in isomer 2 compared to 1.01 Å in isomer 1. In line with the increase in the O−H length of the attacking water molecule, the Mulliken charges indicate that chlorine nitrate in isomer 2 is considerably more polarized than in isomer 1. The *net* charge on Cl_1 and O_5 in isomer 2 is 0.14 compared with −0.02 in isomer 1. Also, the total charge on the NO_2 fragment (N_6, O_7, and O_8) is −0.47 in isomer 2 and −0.40 in isomer 1 (Table 4). The formation of two hydrogen bonds to O_8 in isomer 2 would indicate that it is more favorable for any developing negative charge to reside in part on O_8 as opposed to O_5, which in not participating in hydrogen bonding. As a result there is a significant charge separation within the $ClONO_2$ molecule. Conversely, in isomer 1, both O_5 and O_8 are each hydrogen bonded to one water, and thus, the developing negative charge may be partitioned more evenly between O_5 and O_8. Overall, there is marginally less charge transfer from the attacking H_2O to the $ClONO_2$ entity in isomer 2 than in isomer 1 (Table 4).

Ion Pair Structures. In view of the considerable polarization of $ClONO_2$, evident as the number of solvating water molecules in the clusters is increased, we now discuss the formation and stability of ion pairs involving H_2OCl^+ and NO_3^- in such clusters, which are particularly important in understanding the atmospheric reactivity of $ClONO_2$.

$ClONO_2 \cdot (H_2O)_6$. For the clusters up to and including five water molecules, no stable ion pair could be located that was analogous to the reactant structures that we have identified. As far as clusters containing six water molecules are concerned, isomer 1 (Figure 5) did not lead to a stable ion pair. However, isomer 2 (Figure 6) did lead to a stable ionized structure shown in Figure 7. In this structure, the species HOCl, H_3O^+, and NO_3^- are clearly evident. The strong interaction between HOCl and H_3O^+ and NO_3^- with an O_2-H_3 hydrogen bond distance of 1.59 Å and a nonbonded Cl_1-O_5 distance of 2.30 Å results in considerable distortion of HOCl from the isolated structure (Table 2). Thus, the Cl_1-O_2 intramolecular distance of 1.82 Å is considerably longer than that for free HOCl (1.73 Å). The strong interaction is also evident in the formal charges on the

TABLE 5: Mulliken Charges (*e*) of Core Reaction System (Figure 2) in Ion Pair Structures

	atomic charge		
atom	$ClONO_2 \cdot (H_2O)_6$[a] ($H_3O^+/NO_3^-/HOCl$)	$ClONO_2 \cdot (H_2O)_8$[b] (H_2OCl^+/NO_3^-)	$ClONO_2 \cdot (H_2O)_8$[c] ($H_3O^+/NO_3^-/HOCl$)
Cl_1	−0.03	−0.06	−0.04
O_2	−0.40	−0.37	−0.39
H_3	0.43	0.44	0.34
H_4	0.29	0.40	0.42
O_5	−0.07	−0.05	−0.12
N_6	−0.30	−0.29	−0.30
O_7	−0.05	−0.03	−0.11
O_8	−0.26	−0.15	−0.23
	total fragment charge		
fragment	$ClONO_2 \cdot (H_2O)_6$[a] ($H_3O^+/NO_3^-/HOCl$)	$ClONO_2 \cdot (H_2O)_8$[b] (H_2OCl^+/NO_3^-)	$ClONO_2 \cdot (H_2O)_8$[c] ($H_3O^+/NO_3^-/HOCl$)
NO_3	−0.68	−0.52	−0.76
H_2OCl		0.41	
H_3O	0.75		0.73
HOCl	−0.14		−0.01

[a] Figure 7. [b] Figure 8. [c] Figure 9.

molecular species, being −0.68 on nitrate, 0.75 on hydroxonium, and −0.14 on hypochlorous acid. As far as overall energetics are concerned, the $ClONO_2 \cdot (H_2O)_6$ ion pair structure (Figure 7) and the unionized structure (Figure 6) are essentially isoenergetic (Table 1). In view of this finding, we have studied the structure and energetics of larger structures involving eight water molecules.

$ClONO_2 \cdot (H_2O)_8$. We have investigated two possible arrangements of chlorine nitrate solvated by eight water molecules. The first, shown in Figure 8, is similar to isomer 1 involving six water molecules (Figure 5) but with an additional water molecule inserted into each solvating ring. The eight-water ion pair structure (Figure 8) was obtained from the optimization of an analogous structure containing molecular $ClONO_2$ (Cl_1-O_5 bond length ca. 1.72 Å). In line with the smaller clusters (Figures 4 and 5), the $(H_2O)_8$ structure is related to the rings of waters found on the annealed ice surface studied by Buch et al.[62] Compared to our previous structures, this one shows a further lengthening and shortening respectively of the intra- and intermolecular Cl−O distances, but the formation of a well-defined hypochlorous acid molecule is not seen. The H_2OCl entity has a structure that differs notably from that calculated for the isolated molecule (Table 2). There is thus some lengthening of one of the O−H bonds (O_2-H_3) of the attacking water and reduction in the O_5-N_6 length to 1.33 Å. Further evidence that the reaction is far from completion is afforded by the formal charges, being −0.52 on NO_3 and 0.41 on the H_2OCl entities, respectively (Table 5).

However, a structure that does contain the ionized nitric acid H_3O^+/NO_3^- and HOCl species has been located and identified as a minimum on the potential energy surface (Figure 9). This new ion pair structure was obtained from the first ion pair structure (Figure 8) by a *manual* shift of H_3 from O_2 of the attacking water molecule to the adjacent solvating water molecule. Evidently, from our new ion pair structure (Figure 9), optimization has resulted in a further proton transfer, such that the hydroxonium ion is now adjacent to the nitrate anion. Notably, the hydrogen bonds to the nitrate oxygens have shortened compared with the first ion pair structure, indicating a larger negative charge on the NO_3 species. The chlorine has transferred to form HOCl, where the Cl−O bond length of 1.74 Å is close to that calculated for the isolated structure (Table 2). The nitrate anion and the hydroxonium ion are separated by 1.66 Å, and the Mulliken charges (Table 5) are calculated to be −0.76 on the nitrate and 0.73 on the hydroxonium ion. Importantly, the ion pair is a true energy minimum and does not lead to the spontaneous formation of nitric acid, as indicated in a previous theoretical study by Bianco and Hynes.[38] Energetically, this second ion pair structure (Figure 9) has been found to be more stable than the first ion pair structure (Figure 8) by ca. 1.5 kcal mol.$^{-1}$

TABLE 6: Experimental and Calculated Vibrational Frequencies (cm^{-1}) and (in Parentheses) Intensities (km mol^{-1}) for $ClONO_2$, HOCl, and H_2OCl^+

species	assignment	B3LYP/6-311++G(d,p)	CCSD(T)[a]	expt[c]
$ClONO_2$	NO_2 asym str	1800 (396)	1730 (343)	1735 (vs)
	NO_2 sym str	1341 (295)	1298 (254)	1292 (vs)
	ClO′ str	775 (24)	786 (18)	780 (ms)
	NO_2 sciss	819 (174)	813 (164)	809 (s)
	O′N str	551 (63)	560 (56)	560 (s)
	O′NO_2 ip bend	432 (24)	434 (14)	434 (m)
	ClO′N bend	243 (0.3)	256 (0.1)	270 (vvw)
	O′NO_2 op bend	724 (11)	713 (9.0)	711 (w)
	ClONO torsion	132 (0.5)	122 (0.3)	120
HOCl	O−H str	3779 (80)	3618.8[b]	3609.48[d]
	O−H wag	1224 (38)	1243.5[b]	1238.62[d]
	Cl−O str	701 (3.2)	729.6[b]	724.36[d]
H_2OCl^+	Cl−O str	624 (55)		
	H_2O wag	808 (206)		
	H_2O rock	1037 (8.3)		
	H_2O sym bend	1614 (89)		
	O−H sym str	3540 (339)		
	O−H asym str	3625 (420)		

[a] TZ2P basis set.[41] [b] cc-pV5Z basis set.[46] [c] Referenced by Ying and Zhao ($ClONO_2$).[37] [d] Referenced by Koput and Peterson (HOCl).[46]

B. Spectroscopic Comparisons. We turn now to consider the correlation of the predicted vibrational frequencies of our model clusters with the available experimental data. We first compare (Table 6) our calculated harmonic frequencies for $ClONO_2$ and HOCl with the gas-phase data[37,46] and with previous high-level calculations.[41,46] Our calculated values are generally in good agreement with the experimental data, although it can be seen that the CCSD(T)/TZ2P values are somewhat closer to experiment. We now discuss the frequencies of our reactant and ion pair structures with experiment.

Reactant Structures. A reactant structure has been defined as a system in which the chlorine atom has *not* been transferred to the attacking nucleophile, H_2O. A central feature of this study that has been indicated thus far by our reactant structures is the importance of predissociation or ionization along the O_2NO-Cl bond, serving to increase the electrophilicity of the chlorine atom. Evidently, in all our reactant structures, $ClONO_2$ has *not* undergone hydrolysis but shows increasing ionization as the number of solvating waters is increased. We show the calculated frequencies of these reactant structures given in Table 7. As far as chlorine nitrate is concerned, the extent of ionization is clearly mirrored by our calculated vibrational frequencies. The lengthening of the Cl_1-O_5 bond results in a lowering of the Cl_1-O_5 stretching frequency as the chlorine is transferred and an associated shift to higher frequency of the O_5-N_6 stretch as the nitrate ion is formed. During ionization, and transfer of the chlorine atom, there is an associated lengthening of the O−H bonds of the attacking water molecule. As a result, we observe a lowering of the calculated O−H stretching frequency of the nucleophilic water. Banham et al.[14,15] have recorded an IR spectrum of $ClONO_2$ (2×10^{-8} mbar) co-deposited with H_2O (2×10^{-7} mbar) on a gold foil substrate at 80 K. The reported vibrational frequencies (Table 7) are close to those for the gas-

TABLE 7: Experimental and Calculated Vibrational Frequencies (cm^{-1}) and (in Parentheses) Intensities (km mol^{-1}) of Reactant Structures

species	assignment	expt[a]	$ClONO_2 \cdot (H_2O)_3$[c]	$ClONO_2 \cdot (H_2O)_5$[d]	$ClONO_2 \cdot (H_2O)_6$[e] (isomer 1)	$ClONO_2 \cdot (H_2O)_6$[e] (isomer 2)
H_2O (nucleophile)	O−H_4 str		3860 (95)	3340 (1195)	3340 (1039)	3834 (12)
	O−H_3 str		3326 (1089)	3196 (1361)	2890 (2329)	2502 (2709)
$ClONO_2$	NO_2 asym str	1713 (s)	1700 (422)	1649 (74)[b] 1642 (278)[b]	1624 (284)	1613 (427)
	NO_2 sym str	1294 (vs)	1318 (365)	1308 (455)	1306 (486)	1288 (470)
	NO_2 sciss	782 (s)	862 (229)	910 (296)	924 (298)	942 (235)
	Cl−O str	823 (m)	758 (49)	741 (31)	737 (40)	756 (67)
	NO_2 wag	720 (w)	752 (13)	775 (41)	778 (92)[b] 781 (111)[b]	789 (33)
	O′−N str		630 (88)	682 (36)	691 (32)	694 (17)

[a] $ClONO_2$ (2×10^{-8} mbar) and H_2O (2×10^{-7} mbar) co-deposited at 80 K to give a mixed *unreacted* film.[14,15] [b] Vibrational modes characteristic of assignment occur at both frequencies. [c] Figure 3. [d] Figure 4. [e] Figure 5. [f] Figure 6.

TABLE 8: Experimental and Calculated Vibrational Fequencies (cm^{-1}) and (in Parentheses) Intensities (km mol^{-1}) of Ion Pair Structures

species	assignment	expt A[a]	expt B[b]	$ClONO_2 \cdot (H_2O)_6$[h] ($H_3O^+/NO_3^-/HOCl$)	$ClONO_2 \cdot (H_2O)_8$[i] (H_2OCl^+/NO_3^-)	$ClONO_2 \cdot (H_2O)_8$[j] ($H_3O^+/NO_3^-/HOCl$)
H_2OCl^+	O−H str	3300			2914 (2148) 2322 (3391)	
	H_2O deform	1650			1408 (51)	
	O−Cl str				484 (285)	
NO_3^-				1503 (580)	1565 (381)	1488 (500)
	NO_2 asym str	1430	1450			
	NO_2 asym str	1305	1305	1292 (629)	1302 (622)	1311 (813)
	NO_2 sym str	1040	1032	1062 (55)	1001 (224)	1079 (55)
	NO_3^- op bend		815	845 (45)	803 (19)	825 (21)
H_3O^+	O−H str		3300	3014 (874)[d] 2610 (1600)[e] 2413 (2861)[e]		3235 (864)[f] 3081 (519)[e] 1945 (3067)[g]
	H_3O^+ deform		1750	1740 (7) 1772 (7)		1721 (143)
HOCl[c]	O−H str		2722	3806 (123)		3079 (2083)
	O−H wag			1111 (34) 1129 (83)		1461 (31)
	O−Cl str			537 (199)		674 (53)

[a] RAIR spectrum of $ClONO_2$ (1.5×10^{-6} mbar) and H_2O (1.5×10^{-7} mbar) co-deposited at 180 K.[14,15] [b] RAIR spectrum $ClONO_2$ (3.0×10^{-8} mbar) and H_2O (1.0×10^{-7} mbar) co-deposited at 140/155 K.[17] [c] RAIR spectrum of HOCl on *pure* ice, deposited on substrate at 145 K, bands at, 2716 (O−H str), 1420 (O−H deform), and 725 (Cl−O str).[17] [d] H_3O^+ sym str. [e] H_2O asym str. [f] H_2O sym str. [g] O−H str (longest O−H bond). [h] Figure 7. [i] Figure 8. [j] Figure 9.

phase species (Table 6), confirming that no reaction has taken place. However, they do show small differences that are not systematic. For example, the NO_2 (sciss) and the Cl_1-O_5 stretch are predicted to be at higher and lower frequencies, respectively, in the condensed phase compared to the free molecule situation, as expected, whereas the experimental data show the reverse trend. We find, however, that it is more useful to compare the vibrational frequencies of our ion pair structures with the appropriate experimental data.

Ion Pair Structures. We turn now to the calculated vibrational frequencies (Table 8) of the three ion pair structures (Figures 7−9), all of which differ mainly in the degree to which HOCl is formed and whether it is protonated. Thus, the two structures involving unprotonated HOCl (Figures 7 and 9) have very well developed NO_3^- entities and Cl_1-O_2 lengths that are only slightly longer than those in free HOCl. The structure having protonated HOCl (Figure 8) has a noticeably longer Cl_1-O_2 bond and a corresponding O_5-N_6 bond somewhat longer than the other two. These structural features are reflected in the calculated harmonic frequencies (Table 8). In particular, the frequency of the Cl_1-O_2 stretch correlates well with the Cl_1-O_2 bond length. The calculated predicted decrease in the O−H stretch of HOCl from the isolated molecule (Table 6) to that in the eight water ion pair cluster (Table 8, Figure 8) (700 cm^{-1}) is also in line with the experimental decrease in going from the gas phase (Table 6) to the surface adsorbed species (Table 8, experiment B) (900 cm^{-1}). The other bands observed in experiment can also be well correlated with the calculated frequencies of the $ClONO_2 \cdot (H_2O)_8$ cluster containing the species $H_3O^+/NO_3^-/HOCl$.

The distinguishing feature of experiment A[14,15] (Table 8), is the sharp band at 1650 cm^{-1}, assigned to the H_2O deformation mode of H_2OCl^+. For our structure involving H_2OCl^+ (Figure 8), this frequency is calculated to occur at 1408 cm^{-1}, compared to its value, calculated in free H_2OCl^+, of 1614 cm^{-1} (Table 6).

C. Reactivity of $ClONO_2$. We turn now to consider the atmospheric reactivity of $ClONO_2$. As previously mentioned, experimental investigations,[16,17] indicate that over a range of temperatures (ca. 140−180 K) the hydrolysis reaction leads to the solvated *ionic* nitric and hypochlorous acids, if sufficient surface water is available. In the event of a reduced water concentration at lower temperatures (ca. 140K), the molecular nitric acid ($HONO_2$) is observed, where the reaction is believed to occur via a concerted proton transfer mechanism.[16]

Bianco and Hynes[38] have studied the hydrolysis reaction using the $(H_2O)_3$ reactant structure (Figure 3), at the HF/6-31+G-(d,p) level. The calculated reaction products were found to be

TABLE 9: Electronic and Free Energies (Hartrees) of Stationary Structures for Hydrolysis of $ClONO_2$ in $(H_2O)_6$ Cluster

	B3LYP/6-311++G(d,p)		MP2/6-311++G(d,p)//
structure	electronic energy	free energy (180.0 K)	B3LYP/6-311++G(d,p) electronic energy
$ClONO_2 \cdot (H_2O)_6$[a]	−1199.360336	−1199.220408	−1194.716992
transition state[b]	−1199.359032	−1199.220297	−1194.705850
$ClONO_2.(H_2O)_6$ $(H_3O^+/NO_3^-/$ HOCl)[c]	−1199.362400	−1199.220451	−1199.719560

[a] Figure 6. [b] Figure 10. [c] Figure 7.

the *molecular* nitric and hypochlorous acids. The barrier to reaction was calculated to be ca. 25 kcal mol^{-1}, which dropped to ca. 3 kcal mol^{-1} on the inclusion of electron correlation (MP2 level) and the addition of three solvating STO-3G water molecules. We have studied an analogous reaction involving a three-water cluster similar to the $(H_2O)_3$ reactant structure (Figure 3) at the B3LYP/6-31G(d,p) level. The reaction was found to occur via a concerted proton transfer mechanism leading to the *molecular* nitric and hypochlorous acids, with an activation barrier of ca. 11.4 kcal mol^{-1}. However, at temperatures relevant to the stratosphere (ca. 180 K), the molecular form of nitric acid has never been observed experimentally.[13−17]

In view of the reactant and ion pair structures reported thus far, we have investigated the hydrolysis mechanism linking the $(H_2O)_6$ reactant structure (Figure 6) to the corresponding structure containing the solvated *ionized* nitric and molecular hypochlorous acids (Figure 7). The $(H_2O)_6$ reactant structure was chosen for the study of the hydrolysis reaction for a number of reasons. First, the structural arrangement of the water molecules in the $(H_2O)_6$ reactant structure is closely related to that of hexagonal ice, with two of the surface bilayer waters removed (Figure 1).[55,63] Also, evident from the $(H_2O)_6$ ion pair structure, this structure is capable of stabilizing the ionized nitric acid and thus reproduces the observed reactivity at stratospherically relevant temperatures (ca. 180 K). Finally, we note that the reactivity of $ClONO_2$ could have been investigated using the $(H_2O)_8$ reactant and ion pair structures (Figures 8 and 9). However, the $(H_2O)_6$ reactant and ion pair structures represented a considerable saving of computational expense and were thus preferred. We now discuss the important features of the stationary structures located along the reaction pathway.

The $(H_2O)_6$ reactant structure (Figure 6) in which $ClONO_2$ is significantly ionized has previously been discussed. The most important features are the extended Cl_1-O_5 bond, of length 1.90 Å, and the associated lengthening of the O_2-H_3 bond of the attacking water molecule to 1.04 Å. The corresponding ion pair structure containing H_3O^+, NO_3^-, and HOCl has also been described (Figure 7), in which the strong interaction between HOCl and the ion pair results in a considerable distortion of HOCl from its calculated gas-phase structure. In the absence of thermodynamic corrections, the ion pair structure is found to be more stable than the unionized structure by 1.3 kcal mol^{-1} (B3LYP level) and 1.6 kcal mol^{-1} (MP2 level using the B3LYP geometry). Upon their inclusion, the two structures are essentially isoenergetic (Table 9).

We have located a transition state (Figure 10) connecting the $(H_2O)_6$ reactant and ion pair minima. The transition state is characterized by a single imaginary frequency (322i cm^{-1}), corresponding to a concerted transfer of the chlorine atom from O_5 to O_2 and the transfer of H_3 from O_2 to an adjacent water molecule. An intrinsic reaction coordinate calculation confirmed

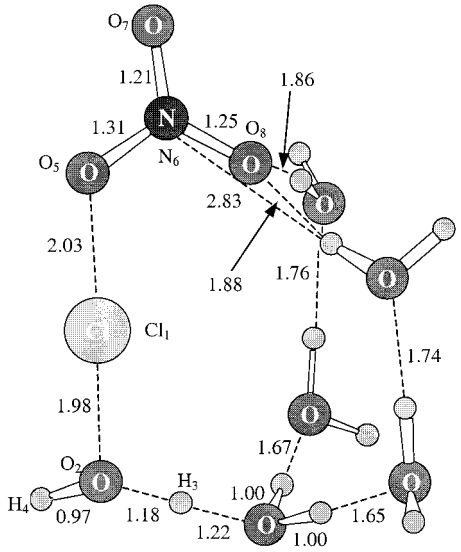

Figure 10. Transition structure linking the $ClONO_2 \cdot (H_2O)_6$ reactant and ion pair structures.

that this was indeed the transition state along the reaction pathway connecting the $(H_2O)_6$ reactant and ion pair structures.

Within the transition structure (Figure 10), the breaking Cl_1-O_5 bond (2.03 Å) of chlorine nitrate is only a little longer than the forming Cl_1-O_2 bond (1.98 Å) of the hypochlorous acid. Also, the breaking O_2-H_3 bond of the attacking water is significantly extended (1.18 Å), while the forming bond of the hydroxonium species is of a similar length (1.22 Å). The associated shortening of the O_5-N_6 bond of the nitrate is well advanced, the O_5-N_6 bond of length 1.31 Å is approximately midway between that of the reactant structure (1.35 Å) and the ion pair structure (1.27 Å). As far as the developing charges on the product ion pair species are concerned, the formal charges associated with NO_3, H_3O, and HOCl of −0.51, 0.64, and −0.18 are close to those associated with the corresponding species in the solvated ion pair structures, namely, NO_3 (−0.68), H_3O (0.75), and HOCl (−0.14).

The barrier for the hydrolysis reaction within the $(H_2O)_6$ reactant structure has been calculated to be 0.8 kcal mol^{-1} at the B3LYP level and 7.0 kcal mol^{-1} at the MP2 level using the B3LYP geometry. The free energy barrier (B3LYP level) is calculated to be essentially zero at 180 K (Table 9). The calculated MP2 barrier is in line with a physiochemical model proposed by Tabazadeh et al.[52] in which the activation energy for the hydrolysis reaction is calculated to be 6.6 kcal $mol.^{-1}$

In view of the calculated low barrier for the hydrolysis reaction in the $(H_2O)_6$ reactant structure, we have investigated the possibility that, by increasing the number of explicit solvating water molecules, the reaction may proceed *without* a barrier. To our $(H_2O)_6$ reactant structure (Figure 6), we have added an additional two *bridging* water molecules hydrogen bonded to O_5 of the nitrate and O_2 of the attacking water molecule, to form a cluster in which $ClONO_2$ is solvated by eight water molecules.

The $(H_2O)_8$ structure containing molecular chlorine nitrate (Cl_1-O_5 bond length ca. 1.72 Å) was optimized at the B3LYP level using a relatively small basis set, namely, 3-21+G(d,p). On optimization, $ClONO_2$ was found to spontaneously ionize leading to the solvated ionic nitric acid and molecular hypochlorous acids, the structure of which is shown in Figure 11. Evidently, from the $(H_2O)_8$ structure, the chlorine atom has transferred to the attacking water molecule, since the intermolecular Cl_1-O_5 distance (2.38 Å) is considerably longer than

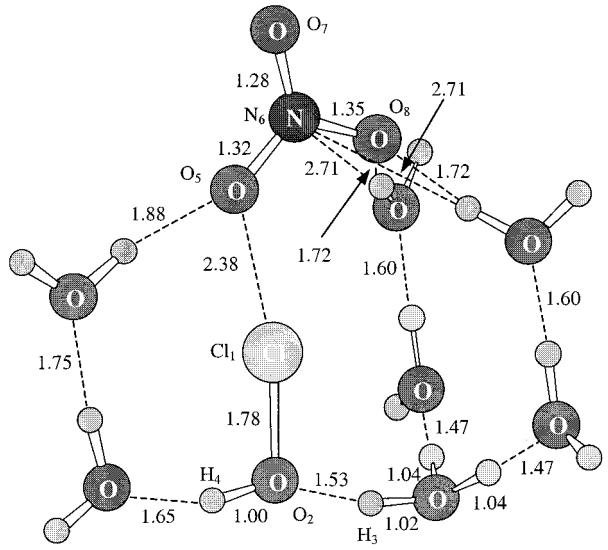

Figure 11. B3LYP/3-21+G(d,p) ion pair structure $ClONO_2 \cdot (H_2O)_8$ showing solvated ionized nitric and molecular hypochlorous acids.

the intramolecular Cl_1-O_2 distance (1.78 Å). The calculated formal charges of the solvated species HOCl (−0.10), NO_3 (−0.78), and H_3O (0.79) indicate significant charge separation and thus suggest that the hydrolysis reaction is complete. Previous calculations involving water clusters have indicted that smaller basis sets can favor ionization,[51] and thus, we have extended these calculations to the larger 6-311++G(d,p) basis set. Calculations on the $(H_2O)_8$ structure using the larger 6-311++G(d,p) basis set also indicate that spontaneous ionization to the solvated ionic nitric and molecular hypochlorous acids occurs. However, the use of a more flexible basis set results in a significant distortion of the smaller basis set structure (Figure 11) involving some structural rearrangement of the solvating waters.

5. Discussion

We first comment on the choice of basis set and the method of including electron correlation. We have shown that density functional theory (B3LYP functional) with the 6-311++G(d,p) basis set gives a chlorine nitrate structure of comparable quality to the CCSD(T)/TZ2P method[41] and is generally in good agreement with the experimental vibrationally averaged gas-phase structure.[41] As far as the water clusters are concerned, we have found that smaller basis sets, namely 3-21+G(d,p), tend to predict preferential stabilization of zwitterionic structures, and thus, in line with previous studies,[51] the larger basis set 6-311++G(d,p) was used in order to more accurately model the potential energy surface.

The calculations described herein reveal a number of important features concerning the mechanism of hydrolysis of $ClONO_2$ on atmospheric aerosols. Our studies support the concept that the reactivity of $ClONO_2$ is controlled by the relative nucleophilic/electrophilic strengths of the species involved. The proposed[16,17] increase in electrophilicity of the chlorine atom of $ClONO_2$, resulting from ionization along the O_2NO-Cl bond, is evident from our reactant structures (Figures 3−6). A lengthening of Cl_1-O_5 and an associated shortening of the O_5-N_6 intramolecular bond clearly shows the catalytic effect of the addition of solvating water molecules, consistent with $ClONO_2$ ionizing toward $H_2OCl^+NO_3^-$. The ionic nature of the interaction between the $ClONO_2$ entity and the water cluster is reflected in the appreciable charge transfer between the attacking water and $ClONO_2$, an effect that increases with the addition of further solvating water molecules. The increasing ionic interaction is also evident from a significant increase in the binding energy of the $ClONO_2$ entity within the water clusters, as the number of solvating water molecules is increased. The extent of ionization of $ClONO_2$ within our unreacted structures is also mirrored by our calculated vibrational frequencies.

Experimentally, at stratospherically relevant temperatures (ca. 180 K), under a low partial pressure of water, RAIR spectroscopic studies[13−15] implicate the existence of an intermediate species H_2OCl^+ in the hydrolysis reaction. The formation of such a species is supported by our unreacted model clusters (Figures 3−6), containing solvated $ClONO_2$, and by the ion pair structure (Figure 8), containing solvated species closely related to NO_3^- and H_2OCl^+. Solvation of $ClONO_2$ in the unreacted clusters with up to six water molecules leads to significant ionization along the O_2NO-Cl bond. However, the addition of two additional water molecules, forming an eight-water cluster (Figure 8), leads to a transfer of the Cl atom to the attacking nucleophile, H_2O, forming a species akin to H_2OCl^+. The developing charges on the NO_3 and H_2OCl entities within this structure indicate that the hydrolysis reaction is far from complete. Thus, the experimental observations[13−15] are explained by considering H_2OCl^+ formation to be the extreme case of ionization (of $ClONO_2$), in which the transferring chlorine atom is closer to the attacking water molecule than to the departing nitrate anion.

Laboratory studies[16] have shown that, if the surface water concentration is increased, the H_2OCl^+ species is rapidly hydrolyzed yielding the solvated HOCl and H_3O^+. For our reactant structures up to and including five water molecules (Figures 3 and 4), no stable ion pairs ($H_3O^+NO_3^-$) could be located. However, for the reactant clusters with $ClONO_2$ solvated by six water molecules, isomer 1 (Figure 5) did not lead to an ion pair, whereas isomer 2 (Figure 6) did lead to a stable ion pair. In the second, six-water isomer (Figure 7), the solvated ion pair ($H_3O^+NO_3^-$) is effectively separated by two solvation shells. Recent ab initio investigations have shown analogous small water clusters to stabilize other ionized acids in this way.[51] For $ClONO_2$ solvated by eight water molecules (Figure 9), the product ion pair ($H_3O^+NO_3^-$) is found to be stable in a ring structure analogous to the smaller water clusters containing three, five, and six (isomer 1) water molecules, but with an additional water molecule inserted into each solvating ring. This structure differs from the six-water ion pair cluster (isomer 2, Figure 7) in that the charged species ($H_3O^+NO_3^-$) are essentially in close contact. The reactivities of the six-water reactant cluster (isomer 2, Figure 6) leading to the stable ion pair ($H_3O^+NO_3^-$, Figure 7) and the eight-water ion pair structure (Figure 9) are in line with experimental observations[13−17] at stratospherically relevant temperatures (ca. 180 K) where only the ionized product, nitric acid ($H_3O^+NO_3^-$), is observed.

These findings indicate that the six-water cluster (Figure 7) is possibly the smallest cluster capable of stabilizing the ion pair species H_3O^+ and NO_3^- and HOCl. The stabilization is assisted by the separation of the ion pair by two solvation shells. Notably, the strong interaction between HOCl and the $H_3O^+NO_3^-$ ion pair also contributes to the stability of theses species in this cluster. As far as the eight-water cluster (Figure 9) is concerned, the net electrostatic stabilization resulting from additional water molecules is a significant contributor to the stability of the ion pair species in this cluster, whereas analogous smaller clusters were unable to stabilize the ion pair.

We turn now to consider the energetics of the hydrolysis reaction. Tabazadeh et al.[52] have predicted a barrier of 6.6 kcal mol^{-1} for the hydrolysis of $ClONO_2$ on PSC aerosols using a physiochemical model. For the reactant structure containing chlorine nitrate solvated by six water molecules (isomer 2, Figure 6), we have shown that the barrier for the hydrolysis reaction to the analogous ion pair structure (Figure 7) is less than 1 kcal mol^{-1} (B3LYP/6-311++G(d,p)) and the free energy barrier (180 K) is essentially zero. These findings suggest that the reaction under stratospheric conditions, where additional waters may be present as part of the ice surface, will proceed effectively without a barrier. Indeed, preliminary calculations using a cluster containing eight water molecules (Figure 11) have indicated the hydrolysis reaction to be spontaneous. Thus, we predict a similar facile hydrolysis reaction on PSC ice aerosol surfaces, where different adsorption sites are available for solvation. Our calculations have also indicated that, for clusters containing *less* than six water molecules, no such facile reactions are predicted leading to either the molecular or ionic products.

Finally, we comment on the water clusters used to model the PSC ice aerosol surface. Combined simulation and experimental investigations by Buch et al.[62] suggest the presence of rings of water molecules of a broad size distribution, where the larger rings are proposed as the sites for acid ionization on icy surfaces. Our reactant structures containing three, five, and six (isomer 1) water molecules (Figures 3−5) could be related to the rings proposed by Buch et al. However, these small structures do not account for the stabilizing effect of the second solvation shell of waters and are unable to accommodate and stabilize the product, ionized nitric acid ($H_3O^+NO_3^-$). In contrast the ring structures involving eight water molecules (Figures 8 and 9), which stabilize the ion pair species, $H_2OCl^+NO_3^-$ and $H_3O^+NO_3^-$, account for the stabilizing effect of the reactive adsorption site and reproduce the observed atmospheric reactivity. The second six-water reactant cluster (Figure 6) has a structure closely related to hexagonal ice (Figure 1).[55,63] The molecular surface structure of a low-temperature hexagonal ice crystal has been probed by Materer et al.;[56] they found that the surface had full bilayer termination. Thus, our model cluster contains a structural arrangement of water molecules representative of the hexagonal ice surface. Notably, the reactive site we have considered contains a surface defect, where adsorption is likely to be more favorable than on the full bilayer terminated surface.

In summary, our investigations have revealed, at a molecular level, the predissociation of $ClONO_2$ leading in the extreme to the formation of a species akin to the $H_2OCl^+NO_3^-$ ion pair. Our range of model clusters have accounted for a number of different adsorption sites likely to be found on the PSC ice aerosol surface. However, our central finding of atmospheric importance[1−12] is that the hydrolysis of $ClONO_2$ can proceed essentially spontaneously in neutral water clusters, of a relatively small critical size, that do not require larger aerosols or clusters containing solvated ionic species.[12]

Acknowledgment. We thank EPSRC for support of this research and Dr. J. C. Whitehead for helpful discussion.

References and Notes

(1) Solomon, S.; Garcia, R. R.; Rowland, F. S.; Wuebbles, D. J. *Nature* **1986**, *321*, 755.
(2) Solomon, S. *Rev. Geophys.* **1988**, *26*, 131.
(3) Solomon, S. *Nature* **1990**, *347*, 347.
(4) Molina, M. J.; Tso, T. L.; Molina, L. T.; Wang, F. C.-Y. *Science* **1987**, *238*, 1253.
(5) Molina, M. J.; Rowland, F. S. *Nature* **1974**, *249*, 810.
(6) Cicerone, R. J. *Science* **1987**, *237*, 35.
(7) Tolbert, M. A. *Science* **1994**, *264*, 527.
(8) Turco, R. P.; Toon, O. B.; Hamill, P. J. *Geophys. Res.* **1989**, *94*, 16493.
(9) McElroy, M. B.; Salawitch, R. J.; Wofsy, S. C. *Geophys. Res. Lett.* **1986**, *13*, 1296.
(10) Henderson, G. S.; Evans, W. F. J.; McConnell, J. C. *J. Geophys. Res.* **1990**, *95*, 1899.
(11) Wennberg, P. O.; Cohen, R. C.; Stimpfle, R. M.; Koplow, J. P.; Anderson, J. G.; Salawitch, R. J.; Fahey, D. W.; Woodbridge, E. L.; Keim, E. R.; Gao, R. S.; Webster, C. R.; May, R. D.; Toohey, D. W.; Avallone, L. M.; Proffitt, M. H.; Loewenstein, M.; Podolske, J. R.; Chan, K. R.; Wofsy, S. C. *Science* **1994**, *266*, 398.
(12) Crutzen, P. J.; Arnold, F. *Nature* **1986**, *324*, 651.
(13) Koch, T. G.; Banham, S. F.; Sodeau, J. R.; Horn, A. B.; McCoustra, M. R. S.; Chesters, M. A. *J. Geophys. Res.* **1997**, *102*, 1513.
(14) Banham, S. F.; Horn, A. B.; Koch, T. G.; Sodeau, J. R. *Faraday Discuss.* **1995**, *100*, 321.
(15) Sodeau, J. R.; Horn, A. B.; Banham, S. F.; Koch, T. G. *J. Phys. Chem.* **1995**, *99*, 6258.
(16) Horn, A. B.; Sodeau, J. R.; Roddis, T. B.; Williams, N. A. *J. Chem. Soc., Faraday Trans.* **1998**, *94*, 1721.
(17) Horn, A. B.; Sodeau, J. R.; Roddis, T. B.; Williams, N. A. *J. Phys. Chem. A* **1998**, *102*, 6107.
(18) Hanson, D. R.; Ravishankara, A. R. *J. Geophys. Res.* **1991**, *96*, 5081.
(19) Hanson, D. R.; Ravishankara, A. R. *J. Phys. Chem.* **1992**, *96*, 2682.
(20) Hanson, D. R.; Ravishankara, A. R. *J. Phys. Chem.* **1994**, *98*, 5728.
(21) Hanson, D. R. *J. Phys. Chem. A* **1998**, *102*, 4794.
(22) Zhang, R.; Jayne, J. T.; Molina, M. J. *J. Phys. Chem.* **1994**, *98*, 867.
(23) Zhang, R.; Leu, M.-T.; Keyser, L. *J. Phys. Chem.* **1994**, *98*, 13563.
(24) Leu, M.-T. *Geophys. Res. Lett.* **1988**, *15*, 17.
(25) Chu, L. T.; Leu, M.-T.; Keyser, L. F. *J. Phys. Chem.* **1993**, *97*, 12798.
(26) Oppliger, R.; Allanic, A.; Rossi, M. J. *J. Phys. Chem. A* **1997**, *101*, 1903.
(27) Tolbert, M. A.; Rossi, M. J.; Malhotra, R.; Golden, D. M. *Science* **1987**, *238*, 1258.
(28) Barone, S. B.; Zondlo, M. A.; Tolbert, M. A. *J. Phys. Chem. A* **1997**, *101*, 8643.
(29) Zondlo, M. A.; Barone, S. B.; Tolbert, M. A. *J. Phys. Chem. A* **1998**, *102*, 5735.
(30) Nelson, C. M.; Okumura, M. *J. Phys. Chem.* **1992**, *96*, 6112.
(31) Van Doren, J. M.; Viggiano, A. A.; Morris, R. A. *J. Am. Chem. Soc.* **1994**, *116*, 6957.
(32) Schindler, T.; Berg, C.; Niedner-Schatteburg, G.; Bondybey, V. E. *J. Chem. Phys.* **1996**, *104*, 3998.
(33) Hatakeyama, S.; Leu, M.-T. *J. Phys. Chem.* **1989**, *93*, 5784.
(34) Hanson, D. R. *J. Phys. Chem.* **1995**, *99*, 13059.
(35) Wofsy, S. C.; Molina, M. J.; Salawitch, R. J.; Fox, L. E.; McElroy, M. B. *J. Geophys. Res.* **1988**, *93*, 2442.
(36) La. Manna, G. *J. Mol. Struct. (THEOCHEM)* **1994**, *309*, 31.
(37) Ying, L.; Zhao, X. *J. Phys. Chem A* **1997**, *101*, 6807.
(38) Bianco, R.; Hynes, J. T. *J. Phys. Chem.* **1998**, *102*, 309.
(39) Akhmatskaya, E. V.; Apps, C. J.; Hillier, I. H.; Masters, A. J.; Palmer, I. J.; Watt, N. E.; Vincent, M. A.; Whitehead, J. C. *J. Chem. Soc., Faraday Trans.* **1997**, *93*, 2775.
(40) Haas, B.-M.; Crellin, K. C.; Kuwata, K. T.; Okumura, M. *J. Phys. Chem.* **1994**, *98*, 6740.
(41) Lee, T. J. *J. Phys. Chem.* **1995**, *99*, 1943.
(42) Lee, T. J.; Rice, J. E. *J. Phys. Chem.* **1993**, *97*, 6637.
(43) Beichert, P.; Schrems, O. *J. Phys. Chem. A* **1998**, *102*, 10540.
(44) Geiger, F. M.; Hicks, J. M.; de Dios, A. C. *J. Phys. Chem. A* **1998**, *102*, 1514.
(45) Robinson Brown, A.; Doren, D. J. *J. Phys. Chem. B* **1997**, *101*, 6308.
(46) Koput, J.; Peterson, K. A. *Chem. Phys. Lett.* **1998**, *283*, 139.
(47) Hanway, D.; Tao, F.-M. *Chem. Phys. Lett.* **1998**, *285*, 459.
(48) Packer, M. J.; Clary, D. C. *J. Phys. Chem.* **1995**, *99*, 14323.
(49) Estrin, D. A.; Kohanoff, J.; Laria, D. H.; Weht, R. O. *Chem. Phys. Lett.* **1997**, *280*, 280.
(50) Vincent, M. A.; Palmer, I. J.; Hillier, I. H.; Akhmatskaya, E. V. *J. Am. Chem. Soc.* **1998**, *120*, 3431.
(51) Smith, A.; Vincent, M. A.; Hillier, I. H. *J. Phys. Chem. A* **1999**, *103*, 1132.
(52) Tabazadeh, A.; Turco, R. P. *J. Geophys. Res.* **1993**, *98*, 12727.
(53) Lee, C.; Vanderbilt, D.; Laasonen, K.; Car, R.; Parrinello, M. *Phys. Rev. B* **1993**, *47*, 4863.
(54) Bernal, J. D.; Fowler, R. H. *J. Chem. Phys.* **1933**, *8*, 515.
(55) Davidson, E. R.; Morokuma, K. *J. Chem. Phys.* **1984**, *81*, 3741.
(56) Materer, N.; Starke, U.; Barbieri, A.; Van Hove, M. A.; Somorjai, G. A.; Kroes, G.-J.; Minot, C. *J. Phys. Chem.* **1995**, *99*, 6267.

(57) Silva, S. C.; Devlin, J. P. *J. Phys. Chem.* **1994**, *98*, 10847.
(58) Devlin, J. P.; Buch, V. *J. Phys. Chem.* **1995**, *99*, 16534.
(59) Delzeit, L.; Powell, K.; Uras, N.; Devlin, J. P. *J. Phys. Chem. B* **1997**, *101*, 2327.
(60) Devlin, J. P.; Buch, V. *J. Phys. Chem. B* **1997**, *101*, 6095.
(61) Rowland, B.; Kadagathur, N. S.; Devlin, J. P.; Buch, V.; Feldman, T.; Wojcik, M. J. *J. Phys. Chem.* **1995**, *99*, 8328.
(62) Buch, V.; Delzeit, L.; Blackledge, C.; Devlin, J. P. *J. Phys. Chem.* **1996**, *100*, 3732.
(63) Casassa, S.; Ugliengo, P.; Pisani, C. *J. Chem. Phys.* **1997**, *106*, 8030.
(64) Morrison, I.; Li, J.-C.; Jenkins, S.; Xantheas, S. S.; Payne, M. C. *J. Phys. Chem. B* **1997**, *101*, 6146.
(65) Moore Plummer, P. L. *J. Phys. Chem. B* **1997**, *101*, 6247.
(66) Moore Plummer, P. L. *J. Phys. Chem. B* **1997**, *101*, 6251.
(67) Frisch, M. J.; Trucks, G. W.; Schlegel, H. B.; Gill, P. M. W.; Johnson, B. G.; Robb, M. A.; Cheeseman, J. R.; Keith, T. A.; Petersson, G. A.; Montgomery, J. A.; Raghavachari, K.; Al-Laham, M. A.; Zakrzewski, V. G.; Ortiz, J. V.; Foresman, J. B.; Cioslowski, J.; Stefanov, B. B.; Nanayakkara, A.; Challacombe, M.; Peng, C. Y.; Ayala, P. Y.; Chen, W.; Wong, M. W.; Andres, J. L.; Replogle, E. S.; Gomperts, R.; Martin, R. L.; Fox, D. J.; Binkley, J. S.; Defrees, D. J.; Baker, J.; Stewart, J. P.; Head-Gordon, M.; Gonzalez, G.; Pople, J. A. *GAUSSIAN94*, revision E.1; Gaussian, Inc.: Pittsburgh, PA, 1995.
(68) Frisch, M. J.; Trucks, G. W.; Schlegel, H. B.; Scuseria, G. E.; Robb, M. A.; Cheeseman, J. R.; Zakrzewski, V. G.; Montgomery, J. A.; Stratmann, R. E.; Burant, J. C.; Dapprich, S.; Millam, J. M.; Daniels, A. D.; Kudin, K. N.; Strain, M. C.; Farkas, O.; Tomasi, J.; Barone, V.; Cossi, M.; Cammi, R.; Mennucci, K.; Pomelli, C.; Adamo, C.; Clifford, S.; Ochterski, J.; Petersson, G. A.; Ayala, P. Y.; Cui, Q.; Morokuma, K.; Malick, D. K.; Rabuck, A. D.; Raghavachari, K.; Foresman, J. B.; Cioslowski, J.; Ortiz, J. V.; Sefanov, B. B.; Liu, G.; Liashenko, A.; Piskorz, P.; Komaromi, I.; Gomperts, R.; Martin, R. L.; Fox, D. J.; Keith, T.; Al-Laham, M. A.; Peng, C. Y.; Nanayakkara, A.; Gonzalez, C.; Challacombe, M.; Gill, P. M. W.; Johnson, B. G.; Chen, W.; Wong, M. W.; Andres, J. L.; Head-Gordon, M.; Replogle, E. S.; Pople, J. A. *GAUSSIAN98*, revision A.1; Gaussian, Inc.: Pittsburgh, PA, 1998.
(69) Lee, C.; Yang. W.; Parr, R. G. *Phys. Rev. B* **1988**, *37*, 785.
(70) Miehlich, B.; Savin, A.; Stoll, H.; Preuss, H. *Chem. Phys. Lett.* **1989**, *157*, 200.
(71) Becke, A. D. *J. Chem. Phys.* **1993**, *98*, 5648.
(72) Møller, C.; Plesset, M. S. *Phys. Rev.* **1934**, *46*, 618.
(73) For more information, see http://www.csar.cfs.ac.uk/.
(74) Obermeyer, A.; Borrmann, H.; Simon, A. *J. Am. Chem. Soc.* **1995**, *117*, 7887.